ELSEVIER

Journal of Organometallic Chemistry 627 (2001) 55–66

Journal of Organometallic Chemistry

www.elsevier.nl/locate/jorganchem

Vibrational spectra and structure of the cyclopentadienyl-anion (Cp^-), the pentamethylcyclopentadienyl-anion (Cp^{*-}) and of alkali metal cyclopentadienyls CpM and Cp*M (M = Li, Na, K)

Éva Bencze [a,b], Boris V. Lokshin [c], János Mink [a,d,*1], Wolfgang A. Herrmann [b], Fritz E. Kühn [b,*2]

[a] *Institute of Isotope and Surface Chemistry, Chemical Research Center, Hungarian Academy of Sciences, P.O. Box 77, H-1525 Budapest, Hungary*

[b] *Anorganisch-Chemisches Institut, der Technischen Universität München, Lichtenbergstr. 4, D-85748 Garching, Germany*

[c] *A.N. Nesmeyanov Institute of Organoelement Compounds, Russian Academy of Sciences, Vavilova str. 28, 117813 Moscow, Russian Federation*

[d] *Department of Analytical Chemistry, University of Veszprém, P.O. Box 158, H-8201 Veszprém, Hungary*

Received 11 January 2001; accepted 16 January 2001

Abstract

Structural, electronical and vibrational properties of Cp^- and Cp^{*-}, and of alkali metal cyclopentadienyl (CpM, M = Li, Na, K) and pentamethylcyclopentadienyl (Cp*M, M = Li, Na) complexes have been studied. The main goals of the study were to investigate the influence of the CH_3 groups on the spectral features and on the M–C force constants and the change of ionic character of the M–C bond for different metals. FT-IR, FT-FIR and FT-Raman spectra of LiCp* and NaCp* compounds were recorded. Density functional theory calculations have been performed in order to obtain optimized geometries, vibrational frequencies and IR intensities. Calculated vibrational data were systematically compared to the experimental ones. Based on the calculations and experimental data, the vibrational spectra of Cp^- and CpM were revised and reinterpreted, and a complete assignment of Cp^{*-} and Cp*Li, Cp*Na vibrations was proposed. Correlations have been determined for the different metal atoms and the charge distribution, bond orders, bond energies and force constants.

Keywords: Cyclopentadienyl complexes; Density functional theory; FTIR; FT-Raman spectroscopy; Normal coordinate analysis

1. Introduction

Cyclopentadienyl complexes are key compounds in the chemistry of π-bonded molecules. In literature, considerable attention has been paid to their vibrational spectra. Spectroscopic analysis allows the elucidation of important information about the metal–ligand bonding, the electron density distribution, the effect of substituents on the metal and ligand, the influence of the oxidation state of the metal, etc.

In comparing the spectra and force fields of complexes with those of the free ligands, important information can be deduced on structural, electronical and vibrational properties of the complexes. The problem is more complicated in the case of the η^5-cyclopentadienyl ligand (Cp) as the spectrum of the free cyclopentadienyl-anion (Cp^-) is unknown. This difficulty may be overcome by the assumption that the Cp^- spectrum is very similar to the ligand spectra in ionic Cp-complexes of alkali metals (CpM). Unfortunately, recording adequate spectra of CpM is relatively difficult due to their pronounced air and moisture sensitivity. Since 1956, attempts have been made to interpret the vibrational spectra of Cp^- and CpM complexes, including normal coordinate analyses (NCA) [1–6]. It was shown that the force field of Cp^- is very similar to that of

[1] *Corresponding author. Tel./fax: +36-1-3922551; e-mail: mink@iserv.iki.kfki.hu

[2] *Corresponding author. Tel.: +49-089-28913108; fax: +49-089-13473; e-mail: fritz.kuehn@ch.tum.de

0022-328X/01/$ - see front matter
PII: S0022-328X(01)00710-0

benzene and the tropilidene cation $C_7H_7^+$. However, most of the NCA work [1–4,6] was based on incomplete or partially incorrectly interpreted experimental data of the pioneering authors [3,7,8], or by merely adapting Cp-ring frequencies from ferrocene spectrum.

Another complication in the analysis of the vibrational spectra of CpM compounds is their polymer structure in the solid state with bridging metal atoms [9]. The spectra, especially in the low-frequency region, do not correlate with those of the monomeric free CpM molecules. This makes it practically impossible to compare metal–ligand frequencies and force constants in the series of CpM compounds. Solution spectroscopy is also not conclusive. The compounds are only soluble in polar and coordinating solvents, such as tetrahydrofuran (THF) or hexamethylphosphoric triamide (HMPA). Therefore, the solution spectra are partially covered by the strong solvent absorption and changed due to strong solvation and ion-pair formation [10,11]. Very little data is available on pentamethylcyclopentadienyl-anion (Cp^{*-}) and its alkali metal complexes (Cp*M).

On the other hand, quantum mechanical ab initio Hartree–Fock calculations have proven to be a powerful tool in the determination of the structure, harmonic force fields and vibrational spectra for the main-group molecules. However, these calculations are difficult for large molecules, especially for those that contain heavy metal atoms; post-Hartree–Fock methods employed are costly.

Recently, it has been shown that density functional theory (DFT) is a reliable alternative to ab initio methods in structure and force field calculations. As a rule, reliable vibrational frequencies can be obtained without scaling procedures and at a considerably lower cost, even for big molecules, containing heavy transition metal atoms [12,13]. Until now, only one publication has appeared concerning the DFT calculations of vibrational spectra of the Cp compounds (Cp^-, CpLi and Cp_2Fe) [14].

In this work, we present the results of systematic investigation, using experimental IR, far infrared (FIR) and Raman observations as well as DFT calculations of the molecular structures, force fields and vibrational spectra for Cp^-, Cp^{*-} and monocyclopentadienyl compounds, CpM and Cp*M, where M = Li, Na, K. The objective of this investigation is to analyze the force fields, obtained by NCA from the experimental spectra and by DFT methods, and to discuss the frequency assignments and regularities in molecular parameters (bond lengths, atomic charges, force constants) as a function of the metal involved and substituents in the ring.

2. Experimental

In the CpM series (M = Li, Na, K), all vibrational spectroscopic experimental data were previously reported in the literature [5,7,10,11].

The synthesis of Cp*Li was achieved by the addition of *n*-butyllithium in hexane to a solution of pentamethylcyclopentadiene in THF [15]. The solid product was separated by filtration, washed with petroleum ether and dried in vacuo. The Cp*Na was purchased from Aldrich as a 0.5 M solution in THF.

The Raman spectra of the Cp* complexes were recorded using a Bio-Rad Digilab dedicated FT-Raman spectrometer using the near-infrared 1064 nm excitation from a Nd:YAG laser. The infrared spectra were measured with a Bio-Rad Digilab FTS-60A system at 4 cm^{-1} resolution in the 4000–400 cm^{-1} region. The FIR measurements (400–50 cm^{-1}) were carried out with the aim of a Bio-Rad Digilab Division FTS-175 spectrometer, using a 6 μm Mylar beamsplitter.

DFT calculations were performed using the DMOL program and the InsightII graphical interface, both produced by Biosym [16]. The Becke88 non-local exchange [17] and the Lee, Yang and Parr [18] (denoted BLYP) non-local correlation gradient corrections were added to the Vosko–Wilk–Nusair local-type correlation functional [19] throughout the calculations. Double numeric basis set with polarization function (DNP) was used, which is comparable to GAUSSIAN 6-31G** basis set. The grid used for numerical integration had an extra fine size (434 angular points/radial shell). In all cases, the non-frozen-core approximation was used.

The geometries of the molecules were fully optimized, until the norm of the gradients became less than 10^{-3} a.u., using the Broyden–Fletcher–Goldfarb–Shanno (BFGS) algorithm [20]. No symmetry constraint has been imposed in the geometry optimization.

The harmonic vibrational frequencies were computed by diagonalizing the mass-weighted second-derivative matrix *F* [21]. The elements of matrix were evaluated by finite differences of analytic gradients, using double-sided displacements of 0.01 Bohr from the optimized geometry for all 3N coordinates. The infrared absorption intensities were calculated from numerical derivatives of the dipole moment vector, using the same displacements. The Cartesian force constants were transformed in internal coordinate force constants by the SUNDIUS program [22].

The NCA calculations were performed using a program reported by Mink et al. [23], which has been updated for IBM-PC compatible computers [24].

3. Results and discussion

3.1. Molecular structures

We were interested in comparing our results with the data of Cp^- and CpLi, reported in the literature [14,26] obtained by different quantum chemical methods (Table 1).

From Table 1 it is obvious that the calculated geometrical parameters show a strong dependence on the method of calculation and on the selected basis set. Semi-empirical methods greatly overestimate the tilt angle of the C–H bonds and the metal-ring distance as well. Nevertheless, there is a good agreement between the metal-ring distances obtained in our work and those obtained by Bérces et al. [14] using DFT calculations and by Pratt and Khan [26] using ab initio 6-311G* calculations. The C–C distances, obtained by DFT non-local approximation differ within the limits of 0.015 Å. All the non-empirical methods show a tilting angle of the C–H bonds away from the metal atom in the range of 0.65–2.60°. This was also observed in ab initio SCF MO calculations of CpLi with various basis sets and fixed C–C, C–H and M-ring distances [29]. The largest basis set used in calculations (4-31G**) gives a tilt angle of 1.91° [29].

To our knowledge, there are no theoretical structure and vibrational calculations of CpNa, CpK and Cp*M complexes in the literature. However, by considering the relatively good agreement between the results of different DFT and ab initio SCF MO calculations for Cp^- and CpLi, we anticipated that the comparison of the results, obtained theoretically with the same approximation for all compounds, can adequately reflect the regularities in the structures of these compounds.

Equilibrium geometries and molecular structural parameters obtained by DFT calculation are presented in Table 2.

The uncoordinated ring of the Cp^- is planar with C–H bonds in the plane of the ring (Table 2). However, the Cp^{*-} contains C–CH_3 bonds that are tilted slightly, possibly due to nonequivalence of C–H bonds of the CH_3 groups. The tilting angles become more pronounced in the Cp and Cp* derivatives, where both the C–H and C–CH_3 bonds bend away from the metal center. It is interesting to note that the variation of the tilting angle shows different trends for Cp*M complexes than for CpM ones. It was proposed [29] that C–H bending is a result of a simple Coulomb effect: such bending puts more negative charge on the face of the ring toward the lithium cation and no covalency is implicated in this effect. This assumption does not contradict our data on the charges of the metal atom in the series of CpM compounds (Table 2). The extent of non-planarity change in the same order as the charges on the metal atom, i.e. Li < K < Na. No such correlation was observed for the tilt angle and the metal charge of Cp*M derivatives. In the Cp*M series the metal charge is the smallest (0.376) and the tilting angle is the largest (5.00°) for the Cp*Li. This result suggests that covalent interaction and, perhaps other factors, like steric interaction, can also be considered as responsible for the C–CH_3 bond deviation from the ring plane.

The other structural parameters for Cp and Cp* compounds, e.g. the charges on the metal and dipole moments, are always higher for the Cp than for the Cp* ones. This indicates a more ionic metal–ligand bond character for CpM complexes than for Cp*M derivatives.

The MCp* series show shorter metal bonds and longer C–C bonds than the corresponding CpM complexes, which is indicative of stronger M–Cp* covalent bonding. In contrast, the dissociation energies are higher for CpM complexes. This finding illustrates that

Table 1
Equilibrium geometrical parameters of Cp^- and CpLi calculated by different quantum chemical methods (bond lengths in Å and bond angles in (°)

	Cp^-		CpLi					
	This work	Ref. [14] [a]	This work	Ref. [14] [a]	Ref. [26] [b]	Ref. [26] [c]	Ref. [26] [d]	Ref. [26] [e]
r(C–C)	1.426	1.418	1.430	1.421	1.467	1.415	1.409	1.427
r(C–H)	1.095	1.096	1.091	1.092				
r(M–C)			2.126	2.123				
r(M-ring)			1.744	1.745 [f]	1.698	1.688	1.749	1.957
Tilt (°)	0		0.65	2.60	1	1	1.52	10

[a] DFT-local density approximation (LDA) augmented by non-local (NL) corrections (denoted LDA/NL) to exchange (Becke88) and correlation (Perdew [27],) denoted BP; Slater-type basis set [28]; frozen-core approximation.
[b] DMOL-min, a minimal basis set with frozen inner core orbitals.
[c] DMOL-DNP, frozen core approximation.
[d] Ab initio/GAUSSIAN with 6-311G* basis set.
[e] PM3 semiempirical method.
[f] Calculated from author's data [14].

Table 2
Calculated (DMOL, BLYP/DNP) bond lengths (Å) and bond angles (°), charges on the metal atom (electron charges), dipole moments (debye), and dissociation energies (kcal mol^{-1}) for Cp^-, Cp^{*-}, CpM and Cp*M (M = Li, Na, K)

	Cp^-	CpLi	CpNa	CpK	Cp^{*-}	Cp*Li	Cp*Na	Cp*K
r(C–C)	1.426	1.430	1.430	1.427	1.430	1.437	1.438	1.434
r(C–H)	1.095	1.091	1.093	1.093				
r(C–H_3) [a]					1.106	1.108	1.108	1.115
[b]					1.107	1.101	1.104	1.105
r(C–CH_3)					1.511	1.514	1.515	1.515
r(M–C)		2.126	2.520	2.870		2.112	2.507	2.837
r(M-center)		1.744	2.207	2.601		1.722	2.188	2.561
α(CCH)	126	125.99	125.97	125.98				
α(CCH_3) [a]					114.05	111.81	112.78	112.87
[b]					112.07	112.16	112.14	112.41
α(CCC(H_3))					126.04	125.90	125.93	125.97
C–H tilt	0	0.65	2.74	2.30				
C–CH_3 tilt					0.90	5.00	4.21	2.78
M charge [c]		0.419	0.894	0.843		0.376	0.872	0.815
Dipole moment		3.97	7.79	8.86		3.35	6.68	7.84
Dissociation energy		92.25	61.69	66.79		85.62	51.70	57.38

[a] C–H — H atom of CH_3 group, oriented up relative to the metal atom.
[b] C–H — H atom of CH_3 group, oriented down relative to the metal atom.
[c] Mulliken charges [25].

the additional ionic contribution to the dissociation energy for CpM compounds is more than the energy gained due to the stronger covalent bonding in Cp*M.

Metal-ring and M–C distances increase with increasing metal electropositivity and atomic radii from Li to K. Mulliken charges [25] on the metal atom follow a different order: Li < K < Na. Assuming that the charge on the metal is representative of the bond's ionic character, it can be deduced that the most ionic compounds in each series are CpNa and Cp*Na and not the corresponding potassium derivatives as is usually expected. This is also supported by the calculated dissociation energy values. They are found to be the highest for Li compounds and lowest for sodium.

On the other hand the C–C bond lengths for both Cp and Cp* ligands decrease in the following order: CpLi ≈ CpNa > CpK > Cp^- (the same order for Cp* complexes). The C–C bond lengths in the potassium compounds are very close to those of the corresponding free anions. The metal–ligand bond orders of M–Cp, calculated by Mayer's method [30], are 0.209, 0.034 and 0.026 for LiCp, NaCp and KCp, respectively, which, however suggests that the CpK is the most ionic compound in this series. This apparent contradiction is due to the varying methods of metal charge determination and to the different ionic and covalent contributions to dissociation energies.

3.2. Vibrational spectra

3.2.1. The cyclopentadienyl anion, Cp^-

The calculated and experimental vibrational frequencies for the Cp^- are given in Table 3, together with the generally accepted assignment of the Cp ring vibrations, based on precedent literature [31]. We proposed the reassignment of the spectra of Cp^- as a result of a more detailed experimental and theoretical analysis. Under normal experimental conditions for IR and Raman spectroscopy, free Cp^- cannot exist without a counter cation. Therefore, one should find the most suitable anion–cation pair with the weakest interaction and the smallest ring distortion for assignment of the "free" Cp^- vibrations. Calculated geometrical parameters for the Cp^- is very similar to those obtained for the ring in the CpK complex. The metal–ligand force constants decrease in the following order: Li > Na > K (see Table 6). Vibrational frequencies of the Cp ligand for dissolved CpLi and CpNa (in THF, HMPA complexes exist predominantly as tight ion- or solvent-separated ion pairs) were found to be very close to those of CpK in solid state [10,11]. Thus, the CpK complex should best approximate the vibrational modes of Cp^-. Consequently, our assignment of Cp^- (Table 3) contains mostly the experimental IR and Raman data of solid CpK complex.

The *C–H stretching vibrations* can be assigned clearly from experimental observations. The strongly polarized Raman line at 3088 cm^{-1} should be ν_1 (A_1') and the weak band in solid-state spectrum at 3068 cm^{-1} should correspond to ν_9 (E_2'). The strongest IR band in this region at 3061 cm^{-1} (average wave-number from lattice splitting) refers to ν_5 (E_1') [11]. Our assignment of these frequencies is different from the previous literature values [31].

The *ring C–C stretching modes* ν_2, ν_6 and ν_{10} have been assigned to 1120, 1440 and 1346 cm^{-1} bands,

respectively. The very strong, polarized Raman peak at 1120 cm^{-1} is the symmetric ring breathing mode (A_1'), the medium IR band at 1440 cm^{-1} can be classified into the E_1' species and the strongest Raman line at 1346 cm^{-1} can be interpreted as ν_{10} (E_2'). For all ionic complexes, there were no Raman bands observed in the region of 850–1010 and 1350–3050 cm^{-1}. We therefore believe that the assignments in the previous literature for peaks at 983, 1455 and 1447 cm^{-1} for ν_2, ν_6 and ν_{10} modes, respectively [31] should be revised. The strong IR active band at 1008 cm^{-1} and the weak Raman line at 1070 cm^{-1} have been attributed to *in-plane C–H bending modes* of ν_7 (E_1') and ν_{11} (E_2'), respectively.

Two optically active vibrations are expected for C–H *out-of-plane deformations*, namely the ν_4 and ν_8 modes. The ν_4 (A_2'') IR active vibration was assigned to the band at 686 cm^{-1}. This is the only observable feature in the γ(CH) region (650–850 cm^{-1}) in the spectra of CpLi and CpNa in HMPA solution, where only the solvent-separated ion pairs exist [11]. The HMPA solubilized CpK displayed a single band at 719 cm^{-1} in the Raman spectrum [10] and this can be attributed to the γ(CH) mode (ν_8) of E_1'' species.

For all Cp complexes, the ν_{12} (E_2') in-plane ring deformation mode, α(CCC) always appears at higher frequencies than in the case of benzene (~ 600 cm^{-1}), possibly due to the increased strain of the five-membered ring with respect to the six-membered one. Therefore, we assigned the Raman band of CpLi, CpNa and CpK to the vibration observed at ~ 850 cm^{-1} [10]. This assignment is supported by the DFT calculations. However, there is no Raman band around 565 cm^{-1} [31] for all three complexes.

The remaining three vibrations (ν_3, ν_{13} and ν_{14}) belong to *inactive modes*. Assignment of these vibrations, belonging to A_2' and E_2'' symmetry species, is not trivial. The values for E_2'' modes were predicted from the spectra of compounds with more covalent M–Cp bond character. Due to the symmetry of the ring lowering

Table 3
Calculated and observed fundamental frequencies (cm^{-1}) and infrared intensities (km mol^{-1}) for Cp^- [a]

Symmetry D_{5h}	No. of vibration	Experimental		Calculated			Assignment	PED (NCA)
		Ref. [31]	Solid (Refs. [10,11])	This work	Ref. [14]			
				BLYP/DNP	BP/Slater	NCA		
A_1' (R)	ν_1	3043	3088	3082	3118.6	3088.7	ν(C–H), C–H str.	98r+2R
	ν_2	983	1119	1106	1097.3	1124.6	ν(C–C), ring breath.	98R+2r
A_2' (i.a.)	ν_3		1260	1209	1204.3	1260.3	β(C–H), C–H i.p. bend.	100β
A_2'' (IR)	ν_4	710	686 [b]	626 (115)	629 (217)	704.2	γ(C–H), C–H o.o.p. bend.	100ρ
E_1' (IR)	ν_5	3039	3061	3061 (145)	3098 (78)	3061.9	ν(C–H), C–H str.	98.5r+1.5R
	ν_6	1455	1440	1391 (32)	1392 (7)	1440.9	ν(C–C), C–C str.	98R+17β+1r
	ν_7	1003	1008	972 (32)	973 (38)	1007.0	β(C–H), C–H i.p. bend.	88β+4R
E_1'' (R)	ν_8	625	719	590	620	719.2	γ(C–H), C–H o.o.p. bend.	100ρ
E_2' (R)	ν_9	3096	3068	3038	3071	3068.0	ν(C–H), CH str.	99r+1α
	ν_{10}	1447	1346	1313	1332	1346.2	ν(C–C), C–C str.	92R+25α+4β
	ν_{11}	1020	1070	1024	1012	1070.0	β(C–H), C–H i.p. bend.	101β+2α
	ν_{12}	565	854	817	827	851.9	α(CCC), CCC i.p. def.	74α+19R+5β
E_2'', i.a.	ν_{13}		686	737	749	686.2	γ(C–H), C–H o.o.p. bend.	100ρ
	ν_{14}		600	617	635	598.6	δ(CCC), ring o.o.p. def.	50χ+50ρ

[a] Internal coordinate notation: R — CC stretch, r — CH stretch, β-in-plane (i.p.) C–H deformation, α — change of CCC angle, ρ-out-of-plane (o.o.p.) C–H deformation, χ — ring puckering deformation, R — Raman active, IR — infrared active, i.a. — inactive, PED — potential energy distribution.

[b] Band observed in IR spectra of CpLi and CpNa in HMPA.

from D_{5h} to C_{5v} they gain Raman activity (class E_2). The ν_{14} mode, δ(CCC) shows little or no sensitivity to the counter ion involved and always appears around 600 cm^{-1} [32]. The out-of-plane γ(CH) modes usually appear at ca. $\sim$850 cm^{-1} and decrease to 650–700 cm^{-1} with increasing ionic character of the M–Cp bond. Previous literature values for these ionic compounds have been reported at 700–750 cm^{-1} for γ(CH) modes [32]. Therefore, we expect that the ν_{13} (E_2'') γ(CH) frequency should appear in the same region as the ν_4 (A_2'') one. The solution phase ν_3 (A_2') band is inactive in the IR and Raman spectra for both D_{5h} and C_{5v} symmetries, but it is observed in the solid state spectra of the complexes, occurring at about 1250 cm^{-1}.

Polzer and Kiefer [6] proposed that the literature assignment of ν_{14}, δ(CCC) mode is erroneous and should be corrected. This mode in the benzene spectrum appears at $\sim$400 cm^{-1}. However, the rigidity of the five-membered cycle is higher than that of the six-membered one and thus, the ring puckering frequency should be shifted to higher wave-numbers. The calculated frequencies of E_2'' modes [6] do not correlate with the observed vibrational data of Cp-compounds. The assignment of 841 cm^{-1} band for ν_{13} seems to be too high for ionic Cp-complexes, and another value at 334 cm^{-1} assigned to the ν_{14} vibration seems to be too low. Additional arguments are in favor of our assignments, proposed in Table 3. The results of the DFT frequency calculations gave the values of 737 and 617 cm^{-1} for ν_{13} and ν_{14}, respectively.

According to the assignment discussed above, it can be concluded that the generally accepted assignment, summarized by Nakamoto [31], should be modified for a number of vibrations. We have previously noted some of these discrepancies in our earlier publications [5,10,11]. Fig. 1 summarizes the approximate normal modes and predicted frequencies of the Cp^- vibrations.

The comparison of calculated frequencies with the experimental ones (Table 3) shows that, in spite of relatively large differences between them, the calculations reproduce the Cp^- spectra correctly. For the in-plane modes, the coincidences are in general better than for the out-of-plane ones. The comparison shows that the deviations from the experimental frequencies are different, but have the same order of magnitude. The differences arising between our results and those of Bérces et al. [14] can be explained by the different parameters used in the calculations (basis sets, approximations, integration parameters).

In general, the results of DFT analysis confirm the assignment of the vibrations to the different symmetry species and to the internal coordinates contribution to the vibrational modes.

The results of the normal coordinate analysis for Cp^- are also presented in Table 3. The initial force field taken was similar to that of the benzene and fitted to the experimental frequencies. The vibrational assignments by DFT and NCA calculations are similar. The potential energy distribution (PED) presented in Table 3 has been obtained by NCA calculations.

Table 4 presents force constants obtained by DFT and NCA calculations. There is a significant difference found for the force constants obtained by the different methods. For example, the difference in the CC stretching force constants is about 2×10^2 N m^{-1}. However, this can be explained by examining the differences in the different theoretical methods and problems of experimental observations.

- The DFT force field uses *all* force constants. NCA analysis uses only the "most important" constants, whose values must be significantly bigger than zero. However, sometimes a small change in a force constant leads to a significant change in the frequencies.
- The solution of the inverse vibrational problem in the NCA calculation is not unique and frequently depends on the quality of the initial approximation.
- DFT calculated frequencies differ quite significantly from experimental ones, but reflect correctly the frequency distribution and the relative band intensities in the IR spectra.
- "Free" Cp^- cannot exist without a counter cation. As it is mentioned above, experimental frequencies were taken from CpK complex.

Thus, a direct comparison of the force fields obtained by DFT and NCA methods is meaningless. Comparing the force constants obtained by the same method in the series of the compounds examined can give useful information about the complexes. This is especially interesting for the series of CpM and Cp*M compounds as their molecular geometry cannot be determined by conventional experimental techniques (X-ray diffraction, inelastic neutron scattering, etc.). Moreover, their experimental vibrational spectra, especially in the low-frequency region, do not correspond to the monomeric free CpM or Cp*M molecules.

3.2.2. Vibrational spectra of CpM (M = Li, Na, K)

The results of the DFT calculations for CpM molecules are presented in Table 5 together with the experimental observations. Most of the Cp-ring vibrations were assigned on the basis of Table 3. However, interpretation of the low-frequency region is still uncertain. The assignment of M–Cp vibrations is done on the basis of the spectra of the solid samples with ionic lattice and polymer structures [5,10,11]. Thus, the vibrations correspond to the translational and librational movements of the metal atoms in the lattice. Some changes have been made in the assignments from the literature [5,10,11] about the vibrations of the tight ion pairs in THF and HMPA solutions. While the structures of the tight ion pairs are similar to the free molecules, they are perturbed by strong solvation.

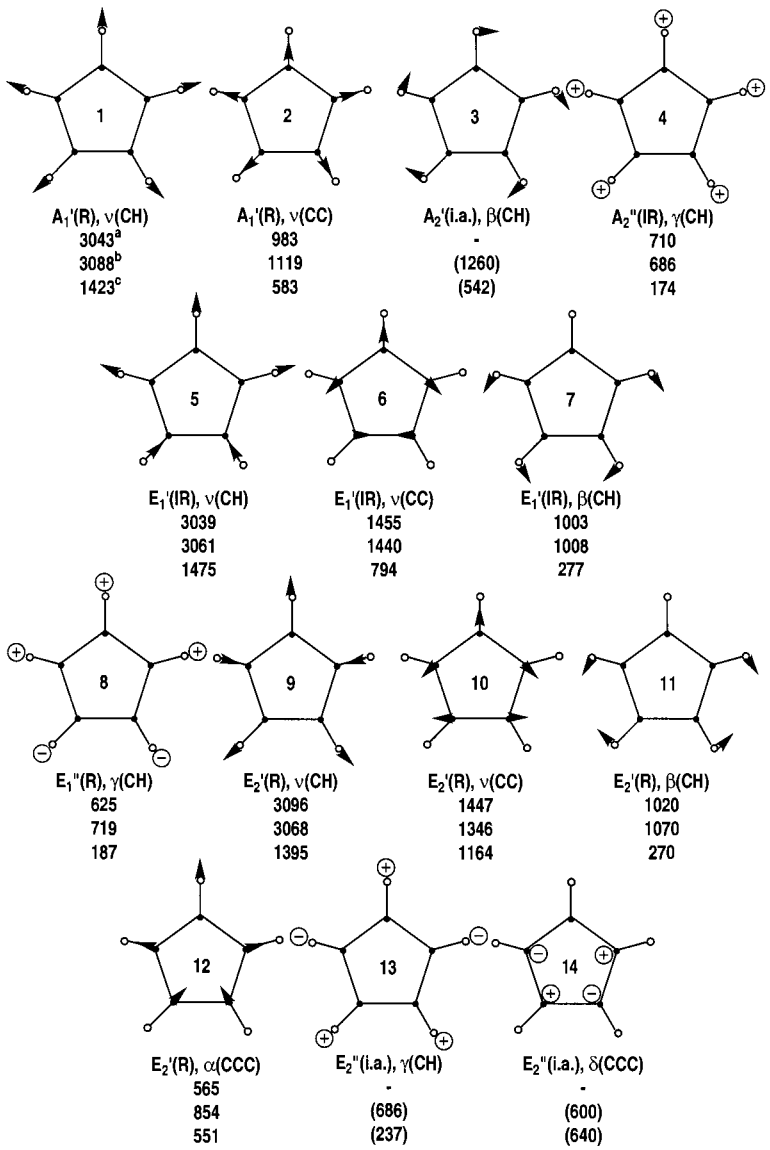

Fig. 1. Approximate normal modes of vibration of the Cp and Cp* groups. Symmetry, band assignments and experimental frequencies (cm^{-1}) of fundamental modes are given. For Cp^{*-} methyl groups were taken as point masses. Notes: (a) experimental frequencies used in Ref. [31]; (b) experimental frequencies referring to Cp^{-}; and (c) experimental frequencies referring to Cp^{*-}.

Table 4
Some diagonal force constants [a] for Cp^{-}, obtained by DFT and NCA calculations

Coordinate	DFT		NCA		
	This work	Ref. [14]	This work	Ref. [5]	Ref. [6]
	(BLYP/DNP)	(BP/Slater)			
r(C–H)	4.375	5.857	6.79	6.97	5.311
R(C–C)	5.164	5.242	5.12	5.42	5.047
α(CCC)	1.236	1.582	1.46	0.97	1.583
β(CCH)	0.411	0.392	0.38	0.43	0.460
γ(C–H), C–H o.o.p. def., ρ	0.294	0.288	0.29		0.245
δ(CCC), ring torsion, χ	0.220	0.584	0.51		0.595

[a] Force constants in 10^2 N m^{-1} for stretching, and in 10^{-18} N m rad^{-2} for bending.

The bands at 515, 430, 365 cm^{-1} (CpLi), 323, 253 cm^{-1} (CpNa) and 213, 173 and 156 cm^{-1} (CpK) in the IR spectra of solid samples [10] are assigned to the translational movements of the metal ions in the lattice. The Raman active bands at ~ 200 cm^{-1} (CpLi), 178 cm^{-1} (CpNa), 180 cm^{-1} (CpK), which show a dependence of the metal atom mass, were assigned to the Cp^- anion tilting modes in the lattice. It is inaccurate to compare these frequencies with the vibrations of the monomeric CpM molecules.

Low-frequency spectra of CpM change dramatically in the transition from the solid state to solution. Unfortunately, CpM complexes only dissolve in polar and strongly coordinating solvents such as THF or HMPA and the solvation of the metal significantly influences the spectra of the molecules. The depolarized Raman bands at 154 cm^{-1} (CpLi), 137 cm^{-1} (CpNa) and 133 cm^{-1} (CpK) in THF solution were assigned to the Cp^- anion tilt in the tight ion pairs and this assignment is used in Table 5 for the ν_{as}(MCp) (E_1) modes [5,10,11].

The FIR solution spectra of CpM show a dependence on the concentration due to the equilibrium between different associates. For CpLi, the band at 426 cm^{-1}, which shows little sensitivity to dilution, was assigned to the M–Cp stretching in the tight ion pair. For CpNa an equilibrium exists between tight and solvent-separated ion pairs in the THF solution. Two bands at 232 and 196 cm^{-1} were observed in the FIR spectrum of the diluted THF solution. The 232 cm^{-1} band decreases in intensity at higher dilution and was therefore assigned to associates. Hence, the 196 cm^{-1} band was assigned to ν_s(CpNa) (A_1) [5,10]. We believe that this assignment should be revised. The spectral feature at 196 cm^{-1} coincides with a band in the spectrum of NaI in THF solution and can be assigned to ν(Na···Solv) vibrations. Therefore, the band at 232 cm^{-1} may indeed correspond to ν_s(CpNa). Considering that in THF solution monomeric molecules are predominant, and that it contains solvent-separated pairs at a concentration of 5×10^{-3} M, used in measurements, the bands at 232 and 196 cm^{-1} can be attributed to ν_s(CpNa) and ν(Na···Solv) vibrations,

Table 5
Experimental and calculated (DMOL; BLYP/DNP) vibrational frequencies (cm^{-1}) and infrared intensities (km mol^{-1}, in parenthesis) of alkali metal cyclopentadienyls CpM (M = Li, Na, K)

Symmetry C_{5v}	No. of vibration	CpLi			CpNa		CpK		Assignment
	(a) (b) [a]	Calc.	Calc. (Ref. [14])	Exp.	Calc.	Exp.	Calc.	Exp.	
A_1	ν_1 1	3141 (0.1)	3158 (17)	3088	3137 (0)	3086	3119 (0)	3088	ν_s(C–H), C–H str.
	ν_2 2	1138 (0.3)	1092 (0)	1114	1136 (1.9)	1119	1143 (0.3)	1119	ν_s(C–C), ring breath.
	ν_3 4	744 (279.8)	730 (365)	735	685 (209.1)	705	694 (193.4)	686	γ(C–H), C–H o.o.p. bend.
	ν_4	564 (16.5)	529 (53)	426	325 (38.8)	232	267 (33.4)	213	ν_s(M–Cp), M–Cp str.
A_2	ν_5 3	1203	1213	1258	1193	1260	1196	1260	β(C–H), C–H i.p. bend.
E_1	ν_6 5	3127 (6.2)	3142 (4)	3080	3122 (15.8)	3061	3103 (23.8)	3061	ν_{as}(C–H), C–H str.
	ν_7 6	1408 (3)	1389 (0)	1433	1408 (6.9)		1416 (5.7)	1440	ν_{as}(C–C), C–C str.
	ν_8 7	992 (33.8)	982 (37)	1006	979 (33.8)	998	980 (30.2)	1008	β(C–H), C–H i.p. bend.
	ν_9 8	721 (4.1)	699 (2)	719	663 (3.3)	715	680 (1.1)	719	γ(C–H), C–H o.o.p. bend.
	ν_{10}	432 (7.4)	372 (0)	154	222 (3.7)	137	208 (1.5)	133	ν_{as}(M–Cp), M–Cp str.
E_2	ν_{11} 9	3110	3112	3078	3104	3061	3084	3068	ν_{as}(C–H), C–H str.
	ν_{12} 10	1382	1328	1346	1378	1342	1386	1346	ν_{as}(C–C), C–C str.
	ν_{13} 11	1023	1030	1067	1013	1062	1013	1070	β(C–H), C–H i.p. bend.
	ν_{14} 12	843	838	854	832	848	828	854	α(CCC), CCC i.p. def.
	ν_{15} 13	826	770	776?	784		795	686	γ(C–H), C–H o.o.p. bend.
	ν_{16} 14	636	602	595	637		629	600	δ(CCC), ring o.o.p. def.

[a] (a) Numbering according to C_{5v} point group for complexes. (b) Numbering referring to D_{5h} point group of the Cp^- (see Table 3).

Table 6
Calculated diagonal force constants [a] of CpM (M = Li, Na, K) complexes

Coordinate	Cp^-	CpLi		CpNa		CpK	
	DFT	DFT	NCA	DFT	NCA	DFT	NCA
R(C–C)	5.164	5.343	6.66	5.288	6.69	5.243	6.71
r(C–H)	4.375	4.257	5.14	4.228	5.10	4.277	5.10
S(C–M)		0.303	0.29	0.230	0.16	0.189	0.08
β(CCH)	0.411	0.415	0.38	0.415	0.39	0.414	0.40
α(CCC)	1.236	1.157	1.48	1.164	1.44	1.181	1.53
γ(C–H), C–H o.o.p. def., ρ	0.294	0.364	0.33	0.351	0.31	0.337	0.31
δ(CCC), ring torsion, χ	0.220	0.214	0.57	0.212	0.53	0.205	0.52

[a] Force constants in 10^2 N m^{-1} for stretching, and in 10^{-18} N m rad^{-2} for bending.

respectively, in the solvated complex CpNa(Solv)$_n$. For CpK, the ν_s(CpK) vibration is assigned to the 213 cm^{-1} band as recorded in solid state FIR spectrum. Therefore, it is clear, that all these assignments are quite tentative, due to the formation of solvated ion pairs CpM(THF)$_n$ significantly altering the MCp frequencies. With complexation of the Cp-anion, the calculated totally symmetric in-plane ν_1, ν_2 and the ν_9 CH out-of-plane vibrations gain IR intensity. The calculated frequencies, the β(CH) in-plane deformations ν_5, ν_7 and ν_{13} are lowered by $\sim$10 cm^{-1}, but all other modes exhibit shifts to high frequency due to the metal "influence". In particular, the CH out-of-plane vibrations (ν_3,ν_9,ν_{15}) showed the greatest high-frequency displacements (50–130 cm^{-1}) as compared to those of the free ligand. The average frequency shifts of +54 and +40 cm^{-1} were obtained for the CH and skeletal CC stretching modes. The in-plane (ν_{14}) and out-of-plane (ν_{16}) CCC skeletal deformations are shifted upwards only by 10–20 cm^{-1}. It is interesting to note that the ν_s(MCp) modes (ν_4) are expected to be much more intense in the IR spectrum than the asymmetric metal–ligand stretching, e.g. the tilt modes (ν_{10}).

In spite of the significant differences between the calculated and experimental frequencies, the theoretically calculated ν(CpM) frequencies and force constants correctly reflect the change in the bond character in the series of alkali metal CpM compounds. This means that it is better to compare the DFT force constants than those calculated by the NCA, as the former are obtained without any preliminary assignment of the experimental spectra. The force constants calculated for CpM by DFT and NCA methods are presented in Table 6 together with those of the Cp^-.

A molecular model was used for the NCA calculation, whereby the movement of the metal in relation to the ring is described by the changes of the five M–C distances, represented by five internal coordinates. From Table 6 it can be seen that the M–Cp force constants calculated by both DFT and NCA methods decrease from Li to K. Most of the other diagonal force constants increase or decrease monotonously from Li to K, except the CH force constants which are the smallest for Na complexes. The decrease of K(CC) corresponds to a lowering of the M–Cp bond orders from Li to K. It has been established empirically [29] that the increase in ionic character of the MCp bond is accompanied by a decrease of the γ(CH) out-of-plane mode frequencies. From Table 5 it can be seen that the γ(CH) frequencies calculated by DFT decrease from Li to Na and then increase from Na to K. The lowest value for Na is in accordance with the highest metal charge and the lowest dissociation energy calculated by DFT (see Table 1). Thus, there is a contradiction in terms of the relative ionic character of the bond, obtained from different structural and spectral characteristics. This problem demands a more detailed study. It is proposed that some of the discrepancies in the complexes are related to different ionic and covalent contributions to the different molecular characteristics.

*3.2.3. The pentamethylcyclopentadienyl anion (Cp^{*-}) and alkali metal pentamethyl-cyclopentadienyls, Cp*M (M = Li, Na, K).*

The calculated (BLYP/DNP) structural parameters of Cp^{*-} and of Cp*M complexes are presented in Table 2 and compared with the Cp complexes (vide supra). It is interesting to note that the average C–C bond length of the ring for the Cp series is 1.428 Å and for Cp^{*-} and the Cp* complexes it is 1.435 Å. The weakening of the ring C–C bond is clearly reflected by the calculated stretching force constants as well (Tables 4 and 9). The metal–carbon distance is shortened by 0.013–0.023 Å in agreement with the higher stability of Cp* complexes in comparison to the Cp ones. The nonplanarity of the Cp ring (C–H tilt) is much stronger for Cp* complexes (C–CH_3 tilt) relative to the Cp derivatives, and among the Cp* series the strongest is found for Cp*Li. This is also an argument of the stronger metal–ligand interaction in the Cp* complexes.

The calculated vibrational spectra for Cp^{*-} and Cp*M are presented in Table 7. To our knowledge

there is no experimental data on Cp*M vibrational spectra in the literature. We recorded the IR and Raman spectra of Cp*Li and Cp*Na. Table 7 summarizes the experimental skeletal vibrations and compares them to the calculated ones. The assignments were made considering the calculated frequencies, IR and Raman intensities of the complexes together with published experimental data on Cp^*_2M (M = Fe(I), Ru(II), Os(III)) complexes [33]. A correct comparison of the calculated and measured frequencies is difficult due, in part, to an overlap of the Cp* ring modes with the deformational modes of CH_3 groups (1300–1500 cm^{-1}). Moreover, the assignment becomes more complex in the low-frequency region, as the ν(M–Cp*) and the ring torsion vibrations appear with the C–CH_3 in-plane and out-of-plane bending modes β(C–CH_3) and γ(C–CH_3). Nevertheless, we tentatively assigned the bands that we believe to be near to the real band positions. The differences between experimental and calculated frequencies are larger in the case of Cp* complexes compared to the Cp ones, possibly due to the bigger size of the ring and the stronger vibrational coupling of the skeletal modes.

The stretching, bending and torsional bands of the CH_3 group are missing in Table 7. The three major features in the CH stretching region can be assigned to asymmetric ($\sim$2965 and $\sim$2950 cm^{-1}) and symmetric 2920 cm^{-1} CH_3 stretching modes. The latest band was observed as polarized line in the Raman spectra of the MCp^*_2 complexes [33]. The asymmetric bendings (1475–1440 cm^{-1}), the symmetric bending ($\sim$1380 cm^{-1}) and the rocking modes (at $\sim$1070 and 1030 cm^{-1}) are observed in the spectral ranges presented in parenthesis.

Theoretical analysis permits us to determine some principal properties of the vibrations of Cp* compounds. In Cp compounds, the most characteristic spectral feature is a very strong and polarized Raman band at $\sim$1100 cm^{-1} of the ring breathing mode. However, this is absent in Cp* complexes. Instead, the Raman spectra highlight two strong and polarized lines of the strongly coupled ring breathing C–C and the total symmetric C–CH_3 vibrations. Due to the proximity of the frequencies, this very strong coupling takes place in all symmetry classes and one of them moves to the high-frequency region 1400–1500 cm^{-1} and another to the low-frequency region ($\sim$600 cm^{-1}). This effect was previously observed in the spectra of Cp^*_2Fe, Cp^*_2Ru, Cp^*_2Os [33].

It is clear that the polarized Raman lines at 1423, 586 and 174 cm^{-1} can be assigned to ν_1, ν_2 and ν_3, respectively (ν_3 becomes Raman active at complexation). The infrared active modes at 1475, 794 and 277 can be assigned to ν_5, ν_6 and ν_7 fundamentals, respectively. The ν_8 is only Raman active for D_{5h} point group, but at complexation (C_{5v} point group) becomes IR active and

Table 7
Experimental and calculated (DMOL, BLYP/DNP) skeletal vibrational frequencies (cm^{-1}) and infrared absorptivities (in km mol^{-1}, in parethesis) of pentamethylcyclopentadienyl anion and of alkali metal pentamethylcyclopentadienyls Cp*M (M = Li, Na, K)

Symmetry species (D_{5h})	Cp^{*-}	Symmetry species(C_{5v})	Cp*Li		Cp*Na		Cp*K	Assignment
	Calc.		Calc.	Exp.	Calc.	Exp.	Calc.	
A_1' (R)	1486	A_1 (IR, R)	1473 (1.8)	1418	1465 (0.8)	1423	1478 (0)	ν_s(C–C)+ν_s(C–CH_3)
	599		598 (0.1)	588	594 (0.6)	583	596 (0.3)	ν_s(C–C)+ν_s(C–CH_3)
A_2'' (IR)	149 (7)		167 (3.5)	169	176 (9.1)	174	134 (0.5)	γ(C–CH_3)
			605 (97.6)	352	353 (59)	318	305 (56.6)	ν_s(M–Cp*)
A_2' (i.a.)	538	A_2 (i.a.)	538	540	538	542	534	β(C–CH_3)
E_1' (IR)	1520 (33)	E_1 (IR, R)	1514 (0)	1379	1503 (1.3)	1475	1518	ν_{as}(C–C)
								+ ν_{as}(C–CH_3)
	804 (1.3)		801 (0.5)	794	795 (0.7)	794	801	ν_{as}(C–C)
								+ ν_{as}(C–CH_3)
	266 (1.2)		243 (2)	276	264 (3.3)	277	262	β(C–CH_3)
E_1'' (R)	250 (1)		287 (14)	185	150 (2.2)	187	94	γ(C–CH_3)
			454 (0.5)	223	316 (1.2)	255	338	ν_{as}(M–Cp*)
E_2' (R)	1463	E_2 (R)	1472	1369	1464	1395	1472	ν_{as}(C–C)
								+ ν_{as}(C–CH_3)
	1181		1181	1059	1178	1164	1180	ν_{as}(C–C)
								+ ν_{as}(C–CH_3)
	261		251	239	250	270	253	β(C–CH_3)
	549		554	555	550	551	549	α(CCC)
E_2'' (i.a.)	137		149	158	141	237	143	γ(C–CH_3)
	632		656	646	655	640	650	δ(CCC)

Table 8
Calculated and observed skeletal fundamental frequencies (cm^{-1}) for Cp^{*-} anion [a]

Symmetry D_{5h}	No of vibration	Experimental (NaCp*)	Calculated BLYP/DNP	NCA	Assignment	PED (NCA)
A_1'	ν_1	1423	1486	1425	ν_s(C–C)+ν_s(C–CH_3), CC str.	53R+47r
	ν_2	583	599	583	ν_s(C–C)+ν_s(C–CH_3), ring breath.	53r+47R
A_2'	ν_3	542	538	542	β(C–CH_3), C–CH_3 i.p. bend.	100β
A_2''	ν_4	174	149	175	γ(C–CH_3), C–CH_3 o.o.p. bend.	100ρ
E_1'	ν_5	1475	1520	1478	ν_{as}(C–C)+ν_{as}(C–CH_3), CC str.	74R+16r+11β
	ν_6	794	804	795	ν_{as}(C–C)+ν_{as}(C–CH_3), C–C str.	90r+7β+3R
	ν_7	277	266	270	β(C–CH_3), C–CH_3 i.p. bend.	90β+9R+r
E_1''	ν_8	187	250	187	γ(C–CH_3), C–CH_3 o.o.p. bend.	100ρ
E_2'	ν_9	1395	1463	1390	ν_{as}(C–C)+ν_{as}(C–CH_3), C–C str.	36R+32β+29r+3α
	ν_{10}	1164	1181	1158	ν_{as}(C–C)+ν_{as}(C–CH_3), CC str.	57r+35r+5β+2α
	ν_{11}	270	261	261	β(C–CH_3), C–CH_3 i.p. bend.	70β+27R+3r
	ν_{12}	551	549	549	α(CCC), CCC i.p. def.	91α+9R
E_2''	ν_{13}	237	137	230	γ(C–CH_3), C–CH_3 o.o.p. bend.	100ρ
	ν_{14}	640	632	640	δ(CCC), ring o.o.p. def.	70χ+30ρ

[a] Internal coordinate notation: R — CC stretch, r — C–CH_3 stretch, β-in-plane (i.p.) C–CH_3 deformation, α — change of CCC angle, ρ-out-of-plane (o.o.p.) C–CH_3 deformation, χ — ring puckering deformation, PED — potential energy distribution.

Table 9
Representative diagonal force constants [a] of Cp* complexes

Coordinate	Cp^{*-}		Cp*Li		Cp*Na		Cp*K [b]
	DFT	NCA	DFT	NCA	DFT	NCA	DFT
R(C–C)	4.659	6.58	4.424	6.49	4.403	6.50	4.545
r(C–CH_3)	4.967	4.94	4.983	5.08	4.916	5.05	4.951
S(C–M)			0.415	0.42	0.291	0.36	0.251
C–H [c]	4.376		4.771		4.679		4.665
[d]	4.659		4.880		4.796		4.782
β(C–CH_3)	0.723	0.43	0.706	0.46	0.715	0.49	0.708
α(CCC)	1.306	1.32	1.201	1.41	1.203	1.37	1.238
HCH [c]	0.487		0.488		0.492		0.490
[d]	0.454		0.444		0.451		0.450
γ(C–CH_3), CH_3 o.o.p. def., ρ	0.079	0.20	0.103	0.25	0.095	0.22	0.075
δ(CCC), ring torsion, χ	0.123	0.50	0.123	0.52	0.120	0.55	0.115

[a] Force constants in 10^2 N m^{-1} for stretching, and in 10^{-18} N m rad^{-2} for bending.
[b] No. of experimental spectra, no. of NCA calculations.
[c] C–H — H atom of the CH_3 group, oriented up relative to the metal atom.
[d] C–H — H atom of the CH_3 group, oriented down relative to the metal atom.

can be observed at 187 cm^{-1}. The only Raman active bands at 1395, 1164, 270 and 551 cm^{-1} can be attributed to ν_9, ν_{10}, ν_{11} and ν_{12} vibrations, respectively. The other inactive modes ν_4, ν_{13} and ν_{14} were observable close to the calculated values as weak features in the solid spectra of Cp*Li and Cp*Na derivatives.

The very strong and polarized Raman bands at 352 and 318 cm^{-1} can be clearly assigned to M–Cp* symmetric stretching modes for Cp*Li and Cp*Na, respectively. The weak IR and Raman line at 223 and 255 cm^{-1} can be attributed to the asymmetric (tilt) metal–ligand stretching modes of Cp*Li and Cp*Na, respectively.

Most of the Cp* ring vibrations exhibit little sensitivity to counter ions, Li and Na. NCA calculations have been made on Cp^{*-} and its alkali metal compounds taking the CH_3 groups as point masses. Table 8 presents the skeletal vibrations and potential energy distribution (PED) of Cp^{*-}. Force constant refinement was made using the experimental frequencies of the NaCp* complex. These results indicate a more powerful mixture of the ring vibrations, very little "pure" C–C,

$C–CH_3$ stretchings and deformations can be obser ved.

The force constants, obtained by DFT calculation are presented in Table 9. The patterns in these values are similar to those found for Cp derivatives. The K(M–Cp*) value decreases from Li to Na to K. Bending force constants χ, ρ, α increase or decrease successively from Li to K. The stretching C–C (ring) and $C–CH_3$ force constants decrease from Li to Na and then increase for K. The HCH bending force constants of CH_3 groups are also minima for Cp*Na.

For all metals studied, the K(MCp*) force constants have higher values, than that for K(MCp). This correlates with a shorter M–Cp* distance and a higher bond order. This does not agree, however, with the lower dissociation energies for all complexes. There is also a contradiction between the experimentally and empirically observed relation of γ(C–H) and the ionic character of the M–C bond. Waterman and Streitweiser [29] stated that as a complex increases in ionic character, the γ(C–H) shifts to lower wave-numbers. DFT calculations show the lowest frequency for this vibration for the Na salts, which correlates with the lowest dissociation energy value and charge on the metal obtained for Na. The force constants always decrease in the order Li > Na > K. The possible origin of all these phenomena was discussed earlier for Cp complexes (vide supra).

4. Conclusions

In both classes of complexes, CpM and Cp*M, the metal–carbon bond orders, the M–Cp(Cp*) distances, the dipole moments and the metal–carbon force constants increase in the order Li > Na > K. The charges on the metals and the dissociation energies are minimum and maximum, respectively for the Na salts. This "anomaly" can be explained by different contributions of the ionic and covalent character of the metal–ligand bonding and the structural and electronic properties of the molecules. The highest covalent character of the metal–ligand bond was obtained for the Li salts (~ 20%).

Acknowledgements

This research was generously supported by operating and equipment grants from the following agencies: Hungarian Academy of Sciences (OTKA, T 025278 and T 016707, AKP 9793-2, 4/29); COST D-5 Brussels, D-246/91, TÉT D-46/98, the Fonds der Chemischen Industrie (financial support). É.B. acknowledges the Alexander von Humboldt Foundation for a fellowship. J.M. is indebted to Alexander von Humboldt Foundation for a Research Award.

References

[1] R.D. Nelson, W.G. Fately, E.R. Lippincott, J. Am. Chem. Soc. 78 (1956) 4870.
[2] L.S. Mayantz, B.V. Lokshin, G.B. Shaltuper, Opt. Spectrosc. 13 (1962) 3317 (in Russian).
[3] A. Sado, R. West, H.P. Fritz, L. Schaefer, Spectrochim. Acta 22 (1966) 509.
[4] J. Brunvoll, S.J. Cyvin, L. Schaefer, J. Organomet. Chem. 27 (1971) 107.
[5] O.G. Garkusha, I.A. Garbuzova, B.V. Lokshin, J. Mink, J. Mol. Struct. 175 (1988) 165.
[6] T. Polzer, W. Kiefer, J. Organomet. Chem. 508 (1996) 153.
[7] H.P. Fritz, L. Schaefer, Chem. Ber. 97 (1964) 1829.
[8] H.P. Fritz, Adv. Organomet. Chem. 1 (1964) 239.
[9] T. Aoyagi, H.M.M. Shearer, K. Wade, G. Whitehead, J. Organomet. Chem. 175 (1979) 21.
[10] I.A. Garbuzova, O.G. Garkusha, B.V. Lokshin, G.K. Borisov, T.S. Morozova, J. Organomet. Chem. 279 (1985) 327.
[11] O.G. Garkusha, I.A. Garbuzova, B.V. Lokshin, G.K. Borisov, J. Organomet. Chem. 336 (1987) 13.
[12] C. Sosa, J. Andzelm, E. Wimmer, K.D. Dobbs, D.A. Dixon, J. Phys. Chem. 96 (1992) 9005.
[13] L. Fan, T. Ziegler, J. Phys. Chem. 96 (1992) 6937.
[14] A. Bérces, T. Ziegler, L. Fan, J. Phys. Chem. 98 (1994) 1584.
[15] F.X. Kohl, D. Kanne, P. Jutzi, Organomet. Synth. 3 (1986) 381.
[16] DMOL 96.0/4.0.0 User Guide, Molecular Simulations, San Diego, CA, September 1996.
[17] A.D. Becke, J. Chem. Phys. 88 (1988) 2547.
[18] C. Lee, W. Yang, R.G. Parr, Phys. Rev. B 37 (1988) 786.
[19] S.H. Vosko, L. Wilk, M. Nusair, Can. J. Phys. 58 (1980) 1200.
[20] H.M. Schlegel, in: K.P. Lawley (Ed.), Ab Initio Methods in Quantum Chemistry-I, Wiley, New York, 1987.
[21] E.B. Wilson, J.C. Decius, P.C. Cross, Mol. Vibrations, Dover, New York, 1980.
[22] T. Sundius, J. Mol. Struct. 218 (1990) 321 (revised in 1997).
[23] J. Mink, J. Kemény, L.M. Mink, Hung. Acad. Sci., Cent. Res. Inst. Phys. KFKI 76-47 (1976) 1.
[24] J. Mink, L. Mink, Computer Program System for Vibrational Analysis of Molecules, Stockholm, 1993.
[25] R.S. Mulliken, J. Chem. Phys. 23 (1955) 1833.
[26] L.M. Pratt, I.M. Khan, J. Comput. Chem. 16 (1995) 1067.
[27] J.P. Perdew, Phys. Rev. B 33 (1986) 8822 (erratum Phys. Rev. B 34 (1986) 7406).
[28] (a) G.J. Snijders, E.J. Baerends, P. Vernooijs, At. Nucl. Data Tables 26 (1982) 483. (b) P. Vernooijs, G.J. Snijders, E.J. Baerends, Slater Type Basis Functions for the Whole Periodic System; Internal Report, Free University of Amsterdam, The Netherlands, 1981.
[29] K.C. Waterman, A. Streitwieser Jr., J. Am. Chem. Soc. 106 (1984) 3138.
[30] I. Mayer, Int. J. Quantum Chem. 29 (1986) 477.
[31] K. Nakamoto, Infrared and Raman Spectra of Inorganic and Coordination Compounds-Part B, fifth ed., Wiley, New York, 1997, p. 286.
[32] V.T. Alexanyan, B.V. Lokshin, J. Organomet. Chem. 131 (1977) 113.
[33] I.A. Garbuzova, A.R. Kudinov, M.I. Rubinskaya, B.V. Lokshin, Metalloorg. Chim. 2 (1989) 922 (in Russian).